Comparing flyover noise measurements to full-scale nose landing gear wind tunnel experiments for regional aircraft

Merino Martinez, Roberto; Neri, Eleonora; Snellen, Mirjam; Kennedy, J; Simons, Dick; Bennett, Gareth J.

DOI
10.2514/6.2017-3006

Publication date
2017

Document Version
Accepted author manuscript

Published in
23rd AIAA/CEAS Aeroacoustics Conference

This is an Accepted Manuscript of an article published in: 23rd AIAA/CEAS Aeroacoustics Conference 5-9 June 2017, Denver, Colorado. ISBN: 978-1-62410-504-3
Available online: https://arc.aiaa.org/doi/10.2514/6.2017-3006

Comparing flyover noise measurements to full–scale nose landing gear wind–tunnel experiments for regional aircraft

Roberto Merino-Martínez*[1], Eleonora Neri†[2], Mirjam Snellen‡[1], John Kennedy§[2], Dick G. Simons¶[1], and Gareth J. Bennett‖[2]

[1] *Delft University of Technology, 2629 HS Delft, the Netherlands*
[2] *Trinity College Dublin, Ireland*

The noise emissions of the nose landing gear of a full–scale model tested in a wind tunnel, and of three regional aircraft types in flyover measurements are compared in this contribution. The geometries of the nose landing gears in all cases were similar. Microphone arrays and beamforming algorithms were used to determine the sound emissions of the nose landing gears. A good agreement was found between the overall trends of the frequency spectra in all cases. Moreover, the expected 6^{th} power law with the flow velocity was confirmed for both experiments. On the other hand, strong tonal peaks (at around 2200 Hz) were only found for the flyover tests. As the frequencies of the tones do not depend on the aircraft velocity, they are thought to be caused by cavities found in structural components of the nose landing gear. Removing these tones would cause overall noise reductions up to 2 dB in the frequency range examined. It is, therefore, recommended to further investigate this phenomenon, to include cavity–noise estimations in the current noise prediction models, and to eliminate such cavities where possible.

I. Introduction

Aircraft noise is one of the major concerns for the aerospace industry and it is an important source of annoyance for the population in the vicinities of airports. Thus, there is an obvious interest in decreasing aircraft noise, as reflected in European organizations, such as ACARE [1] (Advisory Council for Aviation Research and Innovation in Europe) and projects as Flight Path 2050 [2], which aim at reducing the perceived aircraft noise levels by 65% in 2050, with respect to the levels in 2000 (equivalent to a reduction of 15 dB per operation).

During the last decades, turbofan engine noise levels have decreased considerably due to several technological improvements, such as high–bypass turbofan engines and acoustic liners [3]. In this situation, airframe noise can present comparable sound pressure levels (SPL or L_p) as engine noise during the approach stage. One of the major sources of noise in the airframe for commercial aircraft is the landing gear (LG) system [4, 5], which can generate approximately 30% of the whole aircraft noise [6, 7]. The LG system typically consists of complicated structures of bluff bodies (struts, links, wheels, tires, fairings, etc.) of significantly different sizes, which are generally not optimized acoustically.

*PhD candidate, Aircraft Noise & Climate Effects section, Faculty of Aerospace Engineering, Kluyverweg 1. AIAA Student Member. E-mail: r.merinomartinez@tudelft.nl
†PhD candidate, Department of Mechanical and Manufacturing Engineering. AIAA Student Member. E-mail: eneri@tcd.ie
‡Associate professor, Aircraft Noise & Climate Effects section, Faculty of Aerospace Engineering, Kluyverweg 1. E-mail: m.snellen@tudelft.nl
§Assistant Professor, Department of Mechanical and Manufacturing Engineering. E-mail: kennedj@tcd.ie
¶Full professor, Aircraft Noise & Climate Effects section, Faculty of Aerospace Engineering, Kluyverweg 1. E-mail: d.g.simons@tudelft.nl
‖Associate Professor, Department of Mechanical and Manufacturing Engineering. AIAA Senior Member. E-mail: gareth.bennett@tcd.ie

The total landing gear noise consists of the contributions of the nose landing gear (NLG) and the main landing gear (MLG) systems. Even if the MLG is typically larger than the NLG and has a more complex structure (and hence is expected to be noisier), the flow velocity impinging the MLG system is approximately 20% lower than that of the NLG due to the recirculation of the flow underneath the wings [8]. Therefore, the noise levels of both LG systems usually have comparable values [9]. A typical sound signal from a LG system is a combination of broadband noise, mainly caused by the interaction of the LG with the turbulent flow, and tonal noise, generated by noise due to cavities [10, 11] and Aeolian tones due to flow separation and vortex shedding [12, 13]. The frequency of the tone due to a cavity mainly depends on the cavity geometry itself [10], whereas for Aeolian tones, the tone frequency also depends on the flow velocity.

Unfortunately, it is very difficult to model landing gear noise computationally, due to its complex structure and the fact that there are still unknown noise sources present. To obtain a better understanding of the actual noise emissions of LG systems, wind–tunnel [12, 14–17] and aircraft flyover experiments [4, 9] are typically performed. Whereas the first case offers more controlled flow conditions, it requires the LG model being tested to have a high level of geometric detail to represent the small–scale sound generating mechanisms of the gear [4, 5] and it is difficult to replicate the exact conditions present at an aircraft in flight. According to Dobrzynski [5], prediction models based on wind–tunnel tests featuring scale models are prone to underestimate airframe noise levels compared to full–scale flight tests. On the other hand, field experiments with aircraft flyovers under operational conditions present different challenges, such as the inability to control the aircraft position, larger distances between the sound source and the observer, and less–controlled flow characteristics, but they fully represent the actual conditions experienced in reality [18, 19], such as crosswind. Differences between both kinds of experiments typically occur, mostly due to lack of model fidelity, installation effects in the wind tunnel and discrepancies in the Reynolds number [20]. Hence, a comparison between the results of flyover and wind–tunnel measurements is of great interest [13].

For both kind of experiments, a common approach is to employ microphone arrays and beamforming algorithms for estimating the locations and strengths of the sound sources [16, 21–23]. These devices require relatively shorter measurement times compared with other tools, such as acoustic mirrors, enabling cheaper and faster experiments, especially in wind tunnels [24].

The aim of the present paper is to compare the noise emissions of the NLG systems of regional aircraft, measured in a wind tunnel using a full–scale NLG model with those recorded in aircraft flyover measurements. The wind–tunnel experiments were performed under the European Clean Sky funded ALLEGRA (Advanced Low Noise Landing (Main and Nose) Gear for Regional Aircraft) project, coordinated by Trinity College Dublin. This project was developed to assess low–noise technologies applied to a full–scale NLG model [15, 16] and a half–scale MLG model [17] of a regional aircraft. ALLEGRA consisted of a consortium of universities (Trinity College Dublin and KTH), an aeroacoustic wind–tunnel company (Pininfarina SPA), and European SME manufacturing and design partners (Eurotech and Teknosud) supported by a leading landing gear manufacturer (Magnaghi Aeronautica). The field measurements were taken in Amsterdam Airport Schiphol and consisted of 115 aircraft flyovers under operational conditions during the landing stage. Data corresponding to three different regional aircraft types (all equipped with turbofan engines) were selected for this paper.

Both sets of measurements make use of microphone arrays to separate the sound signal emitted at the NLG position. The sound radiation direction considered in this paper corresponds to 90° with respect to the flow direction (vertical direction pointing downwards for flyover measurements). This angle was selected due to the considerably better array performance.

II. Experimental setup

II.A. Wind–tunnel measurements

In the ALLEGRA project the NLG was modeled at full–scale and included a full representation of the LG details and associated structures (e.g., bay cavity, bay doors, belly fuselage and hydraulic dressings). The LG design was obtained from an advanced regional turboprop aircraft design developed as part of the European Clean Sky programme. The models tested within ALLEGRA had a degree of realism not usually found within the literature.

Tests were performed in the Pininfarina open–jet semi–cylindrical aeroacoustic wind–tunnel facility in Turin, Italy, which has a test section of 8 m (length) × 9.60 m (width) × 4.20 m (height). Figure 1 illustrates the relative position of the NLG model in the wind tunnel, as well as the coordinate system employed, where

the xz plane is the symmetry plane of the test model, the yz plane corresponds to the wind–tunnel nozzle exit and the origin is situated in the floor of the testing platform. The full–scale NLG complete model, with the belly fuselage and bay cavities, was positioned in the wind tunnel so that the distance between the wind–tunnel nozzle and the LG wheel axis was 2.8 m. Therefore, the coordinates of the middle point of the wheel axis were:

$$x = 2.8 \text{ m}; \; y = 0 \text{ m}; \; z = 2.175 \text{ m}$$

The wind–tunnel model had a fixed, built–in angle of attack of 4°. Each model configuration was tested at a variety of flow speeds and yaw settings, allowing the analysis of conditions equivalent to landing with a crosswind. For this paper, only the yaw angle of 0° (no crosswind) is considered. Figure 2 shows the overall dimensions of the wind–tunnel test model, whereas Fig. 3 shows a picture of the model inside the wind tunnel.

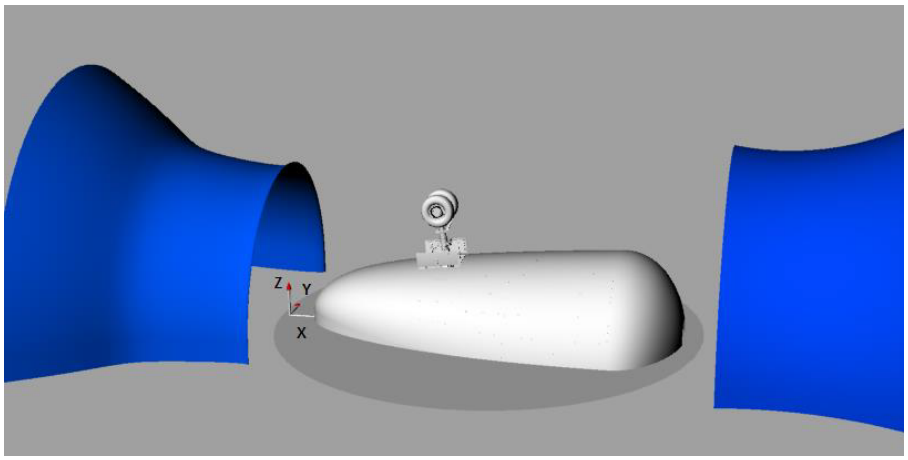

Figure 1: Model and coordinate system inside the Pininfarina wind tunnel

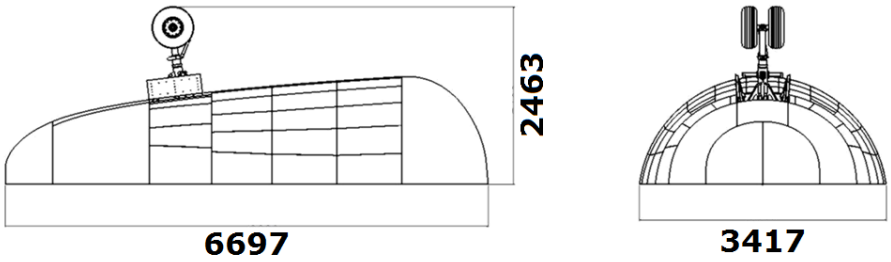

Figure 2: Main dimensions of wind–tunnel test model in mm.

The facility contains a low–noise, high–speed fan–driven system of 13 fans, which provides wind speeds up to 260 km/h (72.2 m/s) and presents a background noise level of 68 dBA at 100 km/h (27.8 m/s). The background noise for the ALLEGRA NLG tests was considered as a combination of the wind–tunnel noise and the noise produced by the belly fuselage itself. Both are mostly low frequency noise sources, below 100 Hz. The flow velocity produced by the wind tunnel is very uniform, since it varies by only 0.5% over the test area. The turbulence level can be adjusted between 0.3% and 8%, using a value of 0.3% in these measurements. Flow velocities of 40, 50, 60 and 65 m/s were selected for the experiment.

Four different planar microphone arrays were installed in the top, side and front of the wind tunnel, which are depicted in Fig. 4. Since only emission angles with respect to the flow direction of 90° are considered in this paper (as well as for the flyover measurements), only the data from the top array are presented here (illustrated with + symbols in Fig. 4). The array had a diameter of 3 m and consisted of 78 microphones. The z coordinate of the array was 4 m, giving a distance to the NLG axis of 1.825 m.

Figure 3: ALLEGRA NLG model inside the wind tunnel.

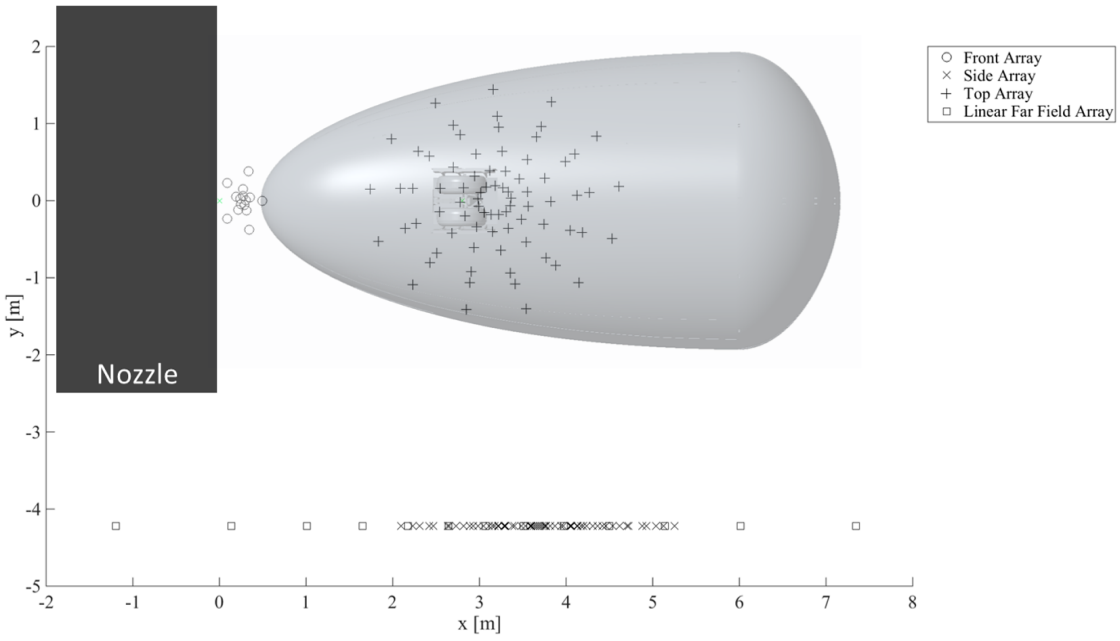

Figure 4: Representation of the location of the top, side and front arrays, as well as the linear far–field array relative to the model and nozzle positions.

Data were acquired simultaneously at all arrays at a sampling frequency of 32,768 Hz for 10 s per measurement. Frequency spectra were processed with a block length of 8192 samples, Hanning windowing and 50% data overlap, providing a frequency resolution of 4 Hz.

The frequency range considered for post–processing ranges from 200 Hz to 4000 Hz. The lower limit was defined by the background noise and the spatial resolution of the array in order to properly separate the sound coming from the NLG model from other noise sources. The higher frequency limit was imposed by the minimum distance between microphones to prevent aliasing, the amount of sidelobes, and the signal–to–noise ratio.

II.B. Flyover measurements

A 32–microphone array with a logarithmic spiral distribution of microphones was situated 1240 m away from the threshold of the Aalsmerbaan runway (36R) in Amsterdam Airport Schiphol, see Fig. 5, after informing the corresponding authorities. The array had an effective diameter of 1.7 m and employed band filters to obtain frequencies between 45 Hz and 11,200 Hz. An optical camera was fixed to the center of the array facing straight up, which provided video footage synchronized with the microphone data. The weather conditions during the measurements were very similar and presented low wind speeds [25].

With this setup, 115 flyovers of landing aircraft were recorded and the respective aircraft types accurately determined. Out of these 115 flyovers, 36 correspond to regional airliners (approximately 31% of the total), showing the importance of regional flights in airports like Amsterdam Airport Schiphol. From all the recorded flyovers, data from three different regional aircraft types were selected for further analysis. Henceforth, for confidentiality reasons, they are referred to as Aircraft Types A, B and C, respectively. The NLG systems from these aircraft types have a similar geometry as the full–scale model tested in the Pininfarina wind tunnel aforementioned, as will be discussed in Sec. II.C.

A sampling frequency of 40 kHz was used. For each measurement, 0.1024 s of data was considered for which the NLG is overhead of the microphone array center (emission angle of 90°, corrected for the source motion). The averaged cross–spectral matrix (CSM) is computed using data blocks of 2048 samples and Hanning windowing with 50 % data overlap, providing a frequency resolution of approximately 20 Hz.

The frequency range selected for further analysis ranges from 1 kHz to 10 kHz. The lower bound was chosen for having enough spatial resolution to separate the sound coming from the NLG position from other noise sources on board, such as the turbofan engines. For the three aircraft types selected, the minimum distance between NLG and engines ranged from 12 m to 20 m, approximately. The fact that Aircraft Types A and C had rear–mounted engines was favorable to separate the contribution of the NLG, see Fig. 7. Aliasing and the amount of sidelobes also determined the highest frequency of study.

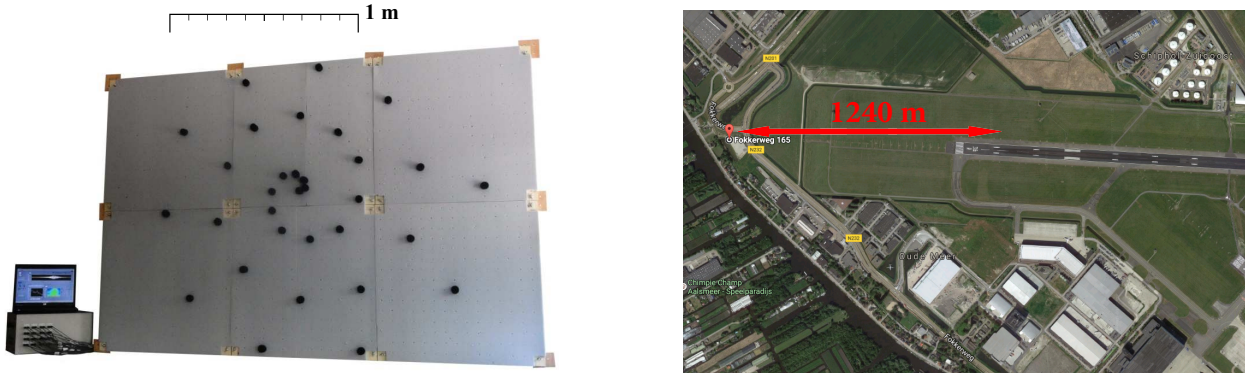

(a) (b)

Figure 5: (a) Configuration of the 32–microphone array; (b) Experimental setup located 1240 m to the South of the threshold of the Aalsmeerbaan (36R) Schiphol airport runway. The North is pointing to the right of the picture.

Approach maneuvers were preferred for this study since the flight trajectories during approach are typically less variable than during takeoff, and especially because, during landing, turbofan engines normally operate at approach idle, making the identification of airframe noise sources (such as the NLG) more likely.

The aircraft trajectories were calculated to account for the propagation effects from the source to the receiver. Data from three different sources [18] were used:

1. The Automatic Dependent Surveillance–Broadcast (when available).
2. The ground radar from air traffic control (provided by Amsterdam Airport Schiphol).
3. The extrapolation of the images taken by the optical camera.

The three methods provided very similar results (with variations up to 6%), but the data from the optical camera were employed due to its availability and because it is easier to overlay the beamforming results to the pictures. The results from the other two methods were used as a validation. The average flight altitude and aircraft velocity above the array for the aircraft studied in this paper were 65.7 m and 69.3 m/s, respectively. Henceforth, true air speeds (considering the wind speeds) are presented.

The background noise contribution was reduced by neglecting all the L_p values under a 30 dB threshold value for each frequency in the spectrograms [25] in order to avoid amplification errors, especially at high frequencies. The Doppler effect was corrected according to Howell *et al.* [26] and the movement of the source was also later considered in the formulation of the beamforming algorithm [18, 24]. Finally, the geometrical spreading and the the atmospheric absorption were also taken into account to obtain the L_p at the source position [3]. A method for calculating the atmospheric absorption coefficient α was employed taking into account the ambient temperature, relative humidity and sound frequency [27].

II.C. NLG geometries

In this subsection, the geometry of the full–scale NLG model tested in the Pininfarina wind tunnel is discussed and compared with the ones of the regional aircraft types selected. All the NLG considered here consist of a single axis and two wheels. Table 1 gathers the dimensions of the tire diameter, tire width and rim diameter for the four NLG geometries, as well as the technical denomination of the NLG (following the ISO metric tire code for flotation sizes) in each case. It can be observed that all the dimensions listed in Table 1 present similar values. Such small differences in the size of the NLG are not expected to cause considerable changes in the L_p values radiated (less than 1 dB) [12].

Table 1: NLG geometries.

Parameter	ALLEGRA	Aircraft Type A	Aircraft Type B	Aircraft Type C
NLG type	22 x 8.0 – 10	24 x 7.7 10 12 PR	24 x 7.7 16 PR	19.5 x 6.75 – 8
Tire diameter, [m]	0.577	0.610	0.610	0.495
Tire width, [m]	0.221	0.196	0.196	0.172
Rim diameter, [m]	0.286	0.305	0.406	0.203

III. Beamforming techniques

III.A. Method for the wind–tunnel experiments

Conventional frequency domain beamforming was applied to the acoustic data of the top microphone array. The beamforming software SAGAS was used for this analysis. This software was developed by DLR, Institute of Aerodynamics and Flow Technology, Department of Experimental Methods, in Göttingen, Germany (Contact: Carsten Spehr). The main diagonal of the CSM was removed in order to eliminate the influence of noise incoherent for all the microphones [24], such as the wind noise. The convection of the sound waves due to the flow velocity was considered. A standard shear layer correction, as outlined by Amiet [28], was applied.

The beamforming results were integrated over an area covering the NLG position, following the approach of the Source Power Integration technique [24]. The beamforming results were normalized by the integrated array response for a point source in the center of the integration area, also known as Point Spread Function (PSF). This way, more physical results are obtained, not conditioned by the assumption that only point sources are present [24, 29–32].

III.B. Method for the flyover measurements

Functional beamforming [33, 34] was selected in this case, as it provides better dynamic range and array spatial resolution than conventional frequency domain beamforming, and these features are very important for flyover measurements, due to the relatively large distance between source and observer [18, 22, 35].

The de–Dopplerized acoustic signals were employed and the movement of the source was taken into account in the beamforming formulation [18, 24, 36]. Removing the main diagonal of the CSM for this algorithm is prone to significant errors, since the method relies on the eigenvalue decomposition of the CSM [37]. For this experiment, however, it was not considered to be necessary to remove the main diagonal of the CSM, due to the low wind speeds and low background noise [18]. This method raises the beamforming source plot to the power of an exponent parameter ν and the CSM to the inverse of this power $\frac{1}{\nu}$. The value of ν chosen to be 32 after performing a sensitivity analysis [18].

Additionally, an integration of the results over an area of interest located at the NLG position for each case was performed (see Fig. 7). The process is similar to the Source Power Integration technique aforementioned, where the beamforming results are now normalized by the PSF at the center of the integration area provided by functional beamforming.

IV. Experimental results

IV.A. Beamforming Results

After applying the SAGAS beamforming method explained in Sec. III.A, different source maps of the ALLEGRA NLG setup were obtained. The scan plane was parallel to the top microphone array, at a distance of 1.825 m from it (containing the wheel axis). Results presented in Figure 6 correspond to a flow speed of 50 m/s and to one–third octave bands with center frequencies of 800 Hz, 1000 Hz and 2000 Hz. The beamforming maps presented have color scales of 10 dB. It is possible to underline how the spatial resolution improves with the increment of the frequency targeted, as expected. The peak of the main lobe appears to be located in the center of the wheel axis. However, sound sources could be located anywhere along the vertical line passing through the middle point of the axis, since the resolution of the microphone array in the z direction is not so accurate to locate the source on the axis, even if the scan plane was defined there. Thus, it is also possible that the main sound source is located on the NLG leg or thereabouts.

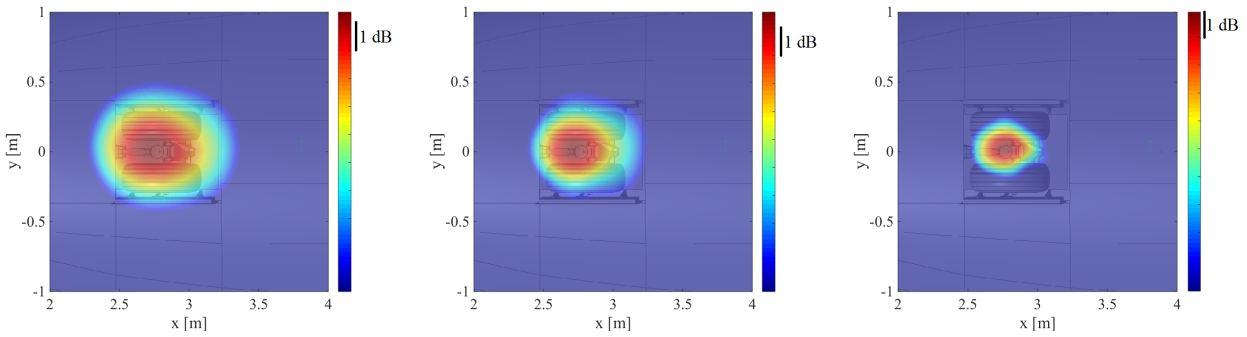

(a) (b) (c)

Figure 6: One–third octave band beamforming source plots for ALLEGRA NLG model at a velocity of 50 m/s and a center frequency of (a) 800 Hz; (b) 1000 Hz; (c) 2000 Hz.

Figure 7 illustrates an example beamforming source plot for a flyover measurement of each of the aircraft types aforementioned. It is observed that the NLG is always the dominant noise source for the frequency range selected (one–third octave band centered at 2 kHz). This frequency band was selected due to the presence of strong tonal noise, as it will be shown in Sec. IV.C. The dashed rectangles denote the integration areas.

For Aircraft Type B (Fig. 7 (b)) an additional sound source is localized at what appears to be the flap side edge of the left wing. For this example the outline of the aircraft has been manually added for clarity, because the sunshine blurred the picture.

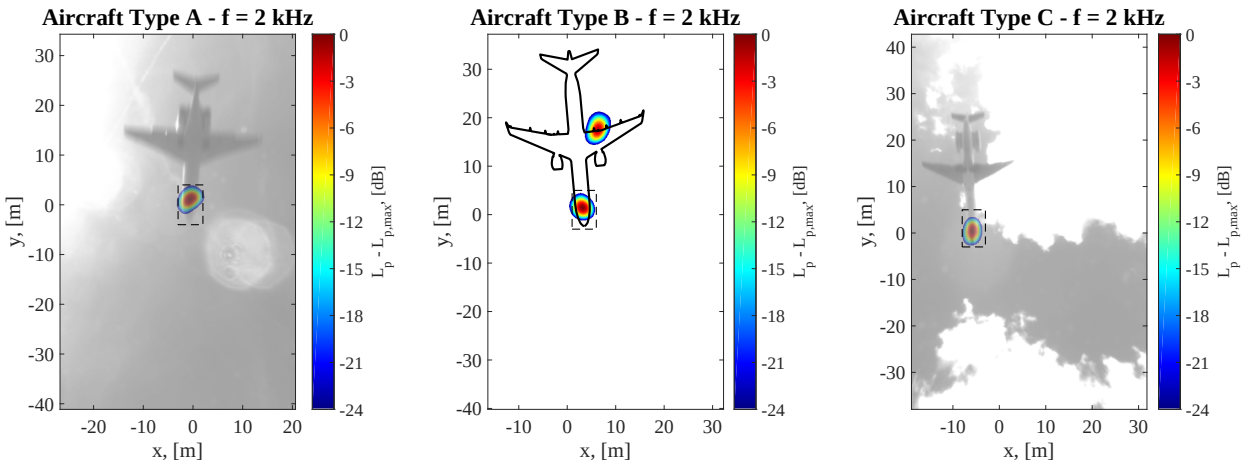

(a) (b) (c)

Figure 7: One–third octave band (2 kHz) beamforming source plots for each aircraft type using functional beamforming with $\nu = 32$. (a) Type A; (b) Type B (aircraft outline has been added for clarity); (c) Type C. The dashed rectangles denote the respective integration areas.

IV.B. Correlation with the flow velocity

Since both datasets considered contain measurements at different flow velocities (or aircraft velocities, for the case of the flyovers), a correlation study is performed to investigate the dependence between the sound pressure level L_p and the flow or aircraft velocity, respectively.

Figure 8 presents the overall L_p (OSPL) values for the available frequency spectra (200 Hz to 4 kHz for the wind–tunnel experiment, and 1 kHz to 10 kHz for the flyover measurements) as a function of the velocity U, using a logarithmic scale for the velocity axis. Results for the ALLEGRA model for the four flow velocities and for the 23 measurements of the Aircraft Type A are presented. This aircraft type was selected due to its higher number of occurrences. A very satisfactory agreement is found between both cases, where the least–squares fits are virtually parallel and almost even coinciding.

The power laws found with respect to the velocity have exponents of 5.90 for the ALLEGRA model and of 5.93 for the Aircraft Type A, see Eq. 1. The variable U_{ref} denotes an arbitrary reference velocity. These values match the 6^{th} power law with velocity expected for NLG noise [4, 5, 12, 38], which considers a compact dipole noise generation mechanism due to unsteady forces [39], assuming that the sound wavelength is comparably larger than the noise source dimensions.

$$L_{p,U} - L_{p,U_{\text{ref}}} \approx \begin{cases} 58.96 \log \frac{U}{U_{\text{ref}}} & \text{for ALLEGRA model} \\ 59.25 \log \frac{U}{U_{\text{ref}}} & \text{for Aircraft Type A} \end{cases} \tag{1}$$

The small differences between both cases are not considered to be statistically significant and are probably explained by the slightly different NLG geometries, the consideration of different parts of the frequency spectrum, and by the different flow conditions in each test case.

Moreover, the statistical coefficients of the correlations are gathered in Table 2, where the correlation coefficient ρ, the coefficient of determination ρ^2 and the $p-$value are presented for each case. An almost perfect fit ($\rho^2 = 0.9999$) is found for the ALLEGRA model, whereas a lower correlation is found for the flyover case ($\rho^2 = 0.7704$). The higher spread of the results for the flyover experiments can be explained due to the less–controlled flow conditions and by possible errors when calculating the true air speeds. Another significant cause of variability is that the 23 measurements correspond to different aircraft, rather than to the same aircraft measured 23 times. In general, both cases present significant correlations if the typical $p-$value threshold of 0.05 is considered. Similar results were found by Snellen *et al.* in [35].

Due to the large dependence between the L_p values generated by the NLG (and most airframe noise sources, in general) and the aircraft velocity, an obvious recommendation would be to reduce the approach speed as much as possible, keeping in mind that the high–lift devices would generate more noise due to the

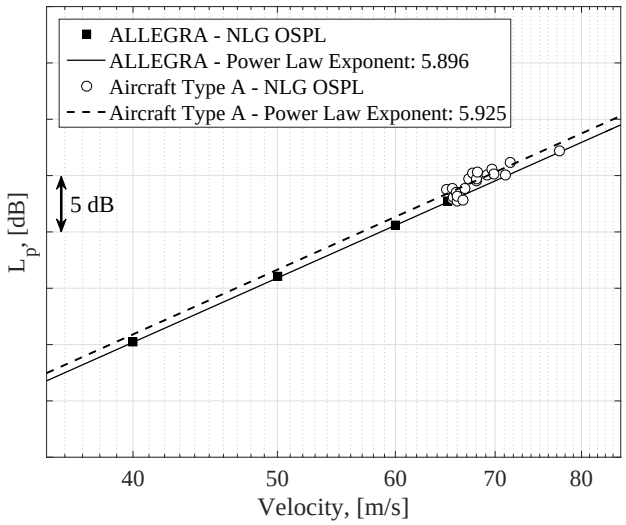

Figure 8: Correlation analysis for the NLG noise of the ALLEGRA model and Aircraft Type A (23 measurements). The least–squares fits are also included. Note the logarithmic scale of the velocity axis.

Table 2: Statistical coefficients for the velocity dependence.

Case	Power law exponent	ρ	ρ^2	p–value
ALLEGRA	5.896	0.9999	0.9999	7.19×10^{-5}
Aircraft Type A	5.925	0.8777	0.7704	3.69×10^{-7}

additional lift requirement.

IV.C. Frequency Spectra Comparison

The narrow–band frequency spectra for the ALLEGRA model for the four flow velocities is presented in Fig. 9 (a), where we can already observe strong similarities within different cases for the whole frequency range available. This fact is further confirmed when the spectra is corrected following the power law with velocity obtained in Eq. 1 taking the 40 m/s as the reference velocity U_{ref}. All the spectra collapse in one single line with only small differences at around 2500 Hz. In general, some tonal components are found for the ALLEGRA model below 500 Hz, but they do not protrude a lot from the high broadband levels around them.

A further comparison between the A–weighted ($L_{p,A}$) frequency spectra (corrected for the velocity influence) of the three different aircraft types is shown in Fig. 10 (a), where the spectrum for the ALLEGRA model at $U = 65$ m/s is plotted for comparison, and that same velocity is taken as a reference U_{ref}. Similar trends are observed between the wind–tunnel and the flyover results, especially for Aircraft Type C. Unfortunately, the region of the spectrum where both wind–tunnel and flyover results overlap is limited (1 kHz to 4 kHz). Other flyover measurements of these aircraft types were similar to the ones presented here, but are not included for the sake simplicity. Since the aircraft velocities are of the same order for the four cases shown in Fig. 10 (a), as well as the NLG geometries, similar Reynolds number are expected to be present.

One can notice that strong tonal noise is present for the three aircraft types at approximately 2200 Hz. This is especially the case for Aircraft Type C, for which a tone, more than 12 dB higher than the broadband noise around it, is found. This phenomenon was already observed for other full–scale aircraft types by Michel and Qiao [4], by Dedoussi *et al.* [13] and by Merino–Martínez *et al.* [9, 18], and for full–scale landing gears of an Airbus A340 in wind–tunnel experiments by Dobrzynski *et al.* [12]. In these publications, it was proposed that the cause for these tonal peaks was the presence of open pin–cavities in the NLG system. For the case of [12], it was determined that one of the main sources of tonal noise was the cavity of the pin that links the brakes and the brake–rods. The fact that no dependency was found between the tone frequency and the

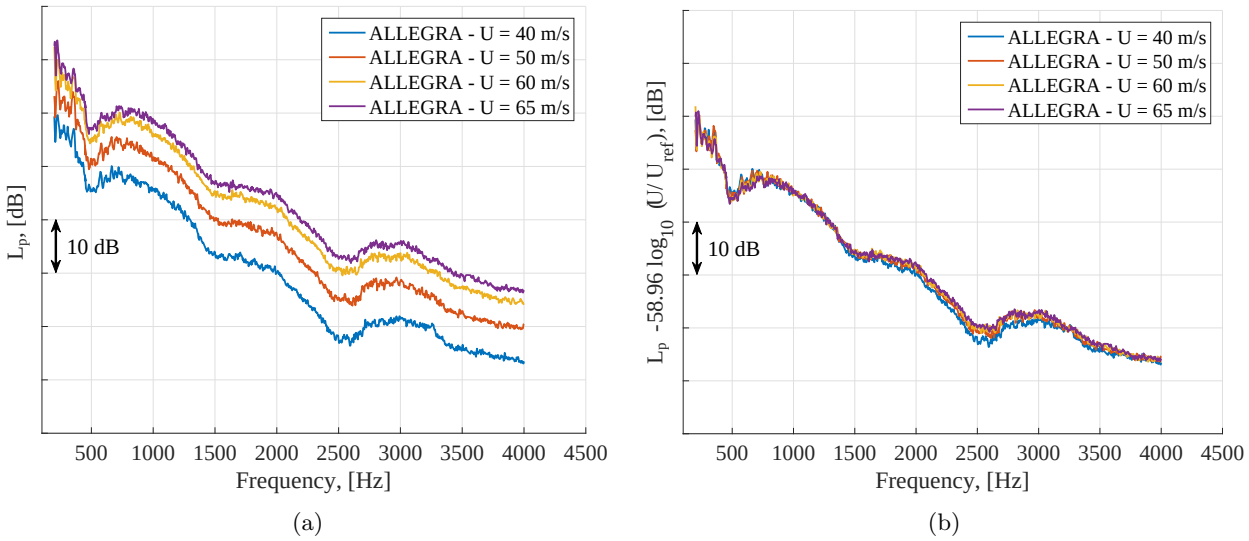

Figure 9: (a) Integrated NLG sound frequency spectra for each velocity of the ALLEGRA model. (b) Idem for the spectra converted to $U_{\text{ref}} = 40$ m/s using the obtained velocity power law.

aircraft velocity (unlike Aeolian tones) also indicates the high probability that the tones originate from a cavity [4, 13]. Since the geometries of the NLG for the three aircraft are similar, it is possible that they have cavities of similar dimensions as well, generating tones with comparable wavelengths. On the other hand, no significant tones were present in the ALLEGRA model in this frequency range. This may be because this cavity tone was designed out of the model.

For the flyover cases, the aforementioned tones were also present in the overall spectra of the whole aircraft, indicating the importance of NLG noise at around 2200 Hz. This is illustrated in Fig. 10 (b) for the same Aircraft Type C flyover measurement as in Fig. 10 (a), where the NLG spectrum is compared to the total aircraft sound spectrum obtained using a single microphone and correcting for the propagation effects [25]. The tone at 2200 Hz is also present in the total aircraft spectrum.

Removing the tone at that frequency would cause overall L_p reductions up to 1 dB (up to 2 dB if A–weighting is considered) for the frequency range considered. In addition, tonal noise is of high importance when assessing aircraft noise around airports, since it has been shown that it causes significantly more annoyance than broadband noise of the same A–weighted sound pressure level [40–42].

Several aircraft noise prediction models do not consider parasitic noise sources, such as cavity noise, in their calculations, which can lead to differences with the measured noise levels [9].

V. Conclusion

Microphone array measurements were performed in both a full–scale nose landing gear system in open–jet wind–tunnel and flyover measurements of three different types of regional aircraft. All the NLG presented similar geometries and an emission angle of 90° is considered for all cases. The overall trends in the sound frequency spectra were similar for both the model tested in the wind tunnel and the three aircraft types. In addition, the increase of sound pressure level with the flow velocity follows the expected 6^{th} power law in both cases.

In the frequency range examined, the NLG was found to be a dominant noise source for all the aircraft flyovers studied, especially around 2200 Hz, where they all presented strong tonal noise components. Since the frequencies of the tones did not depend on the aircraft velocity, the tones are likely to be originated from a cavity. This phenomenon was previously observed in earlier research and is of high importance for the annoyance perceived by population around airports. Moreover, some noise prediction models do not consider cavity noise in their calculations, underestimating the LG noise contribution to the total noise levels. Including cavity–noise estimations in the prediction models would, thus, improve the noise predictions around airports. Cavity noise is considerably difficult to predict since the excitation of the cavity resonant

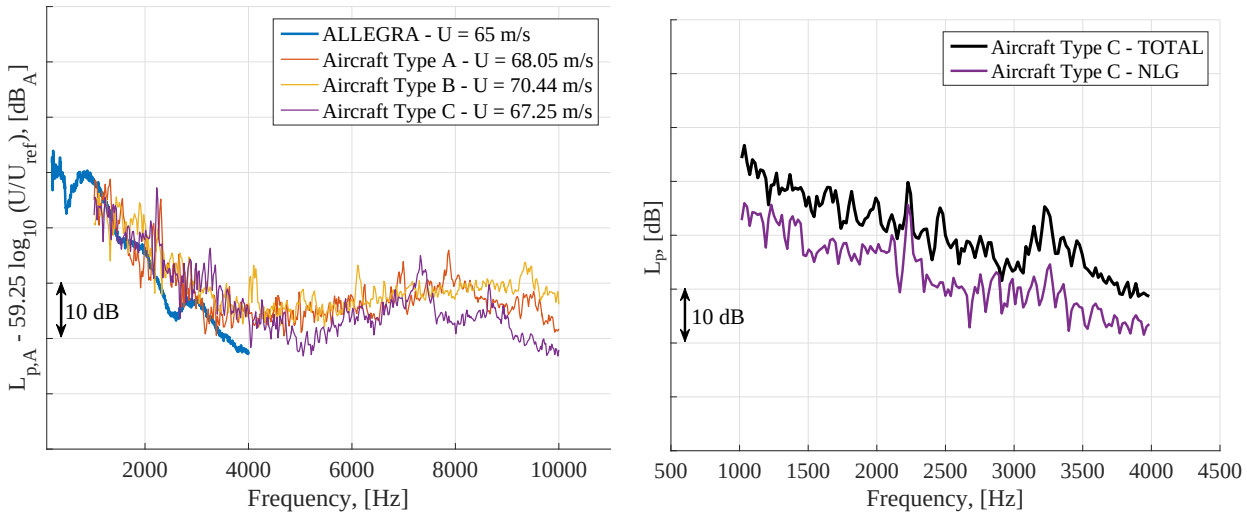

(a) (b)

Figure 10: (a) Integrated A–weighted sound frequency spectra of the NLG for an example flyover of each aircraft type. The spectrum of the ALLEGRA model with $U_{\text{ref}} = 65$ m/s is also plotted for comparison purposes. (b) (Zoomed in) Spectra comparison for an Aircraft Type C flyover between the NLG and the total aircraft ($U = 67.25$ m/s)

mode depends on the velocity, turbulence levels and direction of the flow, but the use of cavity caps might be an effective and easy noise–reduction treatment [12] (keeping in mind practical and safety constraints). On the other hand, the spectra of the NLG model tested in the wind tunnel did not present such strong tones, especially at higher frequencies.

In conclusion, the importance of full–scale aircraft flyover measurements under operational conditions has been confirmed, since they fully represent the circumstances and complex mechanisms of sound generation and propagation experienced in reality. Wind–tunnel measurements, however, are also a necessary research approach, since they provide more controlled flow conditions and allow for parametric studies that would be almost impossible to achieve in flying tests.

Future work includes the assessment of the performance of noise–reduction devices for the NLG [16], such as the aforementioned cavity caps, door spoilers, wheel hub caps, fairings or meshes. Additional studies of the NLG noise emissions on aircraft flyovers with a larger microphone array, and in wind tunnels with more closely–spaced microphones are of high interest, in order to be able to compare the sound spectra over larger frequency ranges.

Acknowledgments

The research leading to the ALLEGRA wind–tunnel results has received funding from the European Union's Seventh Framework Programme (FP7/2007–2013) for the Clean Sky Joint Technology Initiative under grant agreements n° [308225] (ALLEGRA) and n° [620188] (ARTIC). Authors acknowledge all the partners that took part in the ALLEGRA and ARTIC projects. The authors also acknowledge DLR, Institute of Aerodynamics and Flow Technology, Department of Experimental Methods (Contact: Carsten Spehr) for providing the SAGAS software used to generate the wind tunnel beamforming results in this paper.

References

[1] "ACARE – Strategic Research & Innovation Agenda," Tech. rep., 2012.

[2] "Flightpath 2050 Europe's Vision for Aviation," Tech. rep., European Commission, 2012, ISBN 978–92–79–19724–6.

[3] Ruijgrok, G., *Elements of aviation acoustics*, VSSD, Second ed., 2007, ISBN 1090–6562–155–5.

[4] Michel, U. and Qiao, W., "Directivity of Landing–Gear Noise Based on Flyover Measurements," 5^{th} *AIAA/CEAS Aeroacoustics Conference, May 10 – 12 1999, Bellevue, Greater Seattle, WA, USA*, 1998, AIAA paper 1999–1956.

[5] Dobrzynski, W., "Almost 40 Years of Airframe Noise Research: What Did We Achieve?" *Journal of Aircraft*, Vol. 47, No. 2, March–April 2010, pp. 353–367.

[6] Bertsch, L., *Noise Prediction within Conceptual Aircraft Design*, Ph.D. thesis, DLR, 2013, DLR Forschungsbericht, ISRN DLR–FB–2013–20, ISSN 1434–8454.

[7] Piet, J., Molin, N., and Sandu, C., "Aircraft landing gear provided with at least one noise reducing means," U.S. Patent number 8,256,702. 2012.

[8] Pott-Pollenske, M., Dobrzynski, W., Buchholz, H., Guérin, S., Saueressig, G., and Finke, U., "Airframe Noise Characteristics from Flyover Measurements and Predictions," 12^{th} *AIAA/CEAS Aeroacoustics Conference. May 8 – 10 2006. Cambridge, Massachusetts, USA*, 2006, AIAA paper 2006–2567.

[9] Merino-Martinez, R., Bertsch, L., Snellen, M., and Simons, D. G., "Analysis of landing gear noise during approach," 22^{nd} *AIAA/CEAS Aeroacoustics Conference. May 30 – June 1 2016. Lyon, France*, 2016, AIAA paper 2016–2769.

[10] De Metz, F. C. and Farabee, T. M., "Laminar and Turbulent Shear Flow Induced Cavity Resonances," 4^{th} *AIAA Aeroacoustics Conference. October 3 – 5 1977, Atlanta, Georgia, USA*, 1977, AIAA Paper 1977–1293.

[11] Elder, S. A., Farabee, T. M., and De Metz, F. C., "Mechanisms of flow–excited cavity tones at low Mach number," *Journal of the Acoustical Society of America*, Vol. 72, No. 2, August 1982, pp. 532–549.

[12] Dobrzynski, W., Chow, L. C., Guion, P., and Shiells, D., "A European Study on Landing Gear Airframe Noise Sources," 6^{th} *AIAA/CEAS Aeroacoustics Conference. June 12 – 14 2000, Lahaina HI, USA*, 2000, AIAA paper 2000–1971.

[13] Dedoussi, I., Hynes, T., and Siller, H., "Investigating landing gear noise using fly–over data: the case of a Boeing 747–400," 19^{th} *AIAA/CEAS Aeroacoustics Conference, May 27 – 29, 2013, Berlin, Germany*, 2013, AIAA paper 2013–2115.

[14] Dobrzynski, W. and Buchholz, H., "Full–scale noise testing on Airbus landing gears in the German Dutch Wind Tunnel," 3^{rd} *AIAA/CEAS Aeroacoustics Conference. May 12 – 14 1997, Atlanta GA, USA*, 1997, AIAA paper 1997–1597.

[15] Neri, E., Kennedy, J., and Bennett, G., "Characterization of low noise technologies applied to a full scale fuselage mounted nose landing gear," *Proceedings of the Internoise 2015/ASME NCAD Meeting, August 9 – 12 2015, San Francisco, CA, USA*, 2015, NCAD2015–5911.

[16] Neri, E., Kennedy, J., and Bennett, G., "Aeroacoustic source separation on a full scale nose landing gear featuring combinations of low noise technologies," *Proceedings of the Internoise 2015/ASME NCAD Meeting, August 9 – 12 2015, San Francisco, CA, USA*, 2015, NCAD2015–5912.

[17] Kennedy, J., Neri, E., and Bennett, G., "The reduction of main landing gear noise," 22^{nd} *AIAA/CEAS Aeroacoustics Conference. May 30 – June 1 2015. Lyon, France*, 2016, AIAA paper 2016–2900.

[18] Merino-Martinez, R., Snellen, M., and Simons, D. G., "Functional beamforming applied to imaging of flyover noise on landing aircraft," *Journal of Aircraft*, Vol. 53, No. 6, November–December 2016, pp. 1830–1843.

[19] Simons, D. G., Snellen, M., Midden, B., Arntzen, M., and Bergmans, D. H. T., "Assessment of noise level variations of aircraft fly–overs using acoustic arrays," *Journal of Aircraft*, Vol. 52, No. 5, September–October 2015, pp. 1625–1633.

[20] Stoker, R., Guo, Y., Streett, C., and Burnside, N., "Airframe noise source locations of a 777 aircraft in flight and comparisons with past model–scale tests," 9^{th} *AIAA/CEAS Aeroacoustics Conference. May 12 – 14 2003. Hilton Head, South California, USA*, 2003, AIAA paper 2003–3232.

[21] Mueller, T., *Aeroacoustic Measurements*, Springer Science & Business Media, 2002, ISBN–978–3–642–07514–8.

[22] Merino-Martinez, R., Snellen, M., and Simons, D. G., "Functional Beamforming Applied to Full Scale Landing Aircraft," 6^{th} *Berlin Beamforming Conference, February 29 – March 1 2016, Berlin, Germany*, GFaI, e.V., Berlin, 2016, BeBeC–2016–D12.

[23] Merino-Martinez, R., Snellen, M., and Simons, D. G., "Determination of Aircraft Noise Variability Using an Acoustic Camera," 23^{rd} *International Congress on Sound and Vibration, July 10 – 14 2016, Athens, Greece*, 2016.

[24] Sijtsma, P., "Phased array beamforming applied to wind tunnel and fly–over tests," Tech. Rep. NLR–TP–2010–549, National Aerospace Laboratory (NLR), Anthony Fokkerweg 2, 1059 CM Amsterdam, P.O. Box 90502, 1006 BM Amsterdam, The Netherlands, December 2010.

[25] Snellen, M., Merino-Martinez, R., and Simons, D. G., "Assessment of aircraft noise sources variability using an acoustic camera," 5^{th} *CEAS Air & Space Conference. Challenges in European Aerospace. September 7 – 11 2015, Delft, Netherlands*, 2015.

[26] Howell, G. P., Bradley, M. A., McCormick, M. A., and Brown, J. D., "De–Dopplerization and acoustic imaging of aircraft flyover noise measurements," *Journal of Sound and Vibration*, Vol. 105, No. 1, Feb 1986, pp. 151–167.

[27] Arntzen, M., *Aircraft noise calculation and synthesis in a non–standard atmosphere*, Ph.D. thesis, Delft University of Technology, 2014.

[28] Amiet, R., "Refraction of sound by a shear layer," *Journal of Sound and Vibration*, Vol. 58, No. 4, 1978, pp. 467–482.

[29] Kennedy, J., Eret, P., Bennett, G., Sopranzetti, F., Chiarotti, P., Castellini, P., Finez, A., and Picard, C., "The application of advanced beamforming techniques for the noise characterization of installed counter rotating open rotor," 19^{th} *AIAA/CEAS Aeroacoustics Conference. May 27 – 29 2013. Berlin, Germany*, 2013, AIAA paper 2013–2093.

[30] Arce León, C., Merino-Martinez, R., Ragni, D., Avallone, F., and Snellen, M., "Boundary layer characterization and acoustic measurements of flow–aligned trailing edge serrations," *Experiments in Fluids*, Vol. 57, No. 182, October 2016, pp. 22.

[31] Arce León, C., Merino-Martinez, R., Ragni, D., Avallone, F., Scarano, F., Pröbsting, S., Snellen, M., Simons, D. G., and Madsen, J., "Effect of trailing edge serration–flow misalignment on airfoil noise emission," *Journal of Sound and Vibration*, Vol. 405, May 2017, pp. 19 – 33.

[32] Merino-Martinez, R., van der Velden, W. C. P., Avallone, F., and Ragni, D., "Acoustic measurements of a DU96–W–180 airfoil with flow-misaligned serrations at a high Reynolds number in a closed–section wind tunnel," 7^{th} *International Meeting on Wind Turbine Noise, May 2 – 5 2017, Rotterdam, the Netherlands*, 2017.

[33] Dougherty, R. P., "Functional Beamforming," 5^{th} *Berlin Beamforming Conference, February 19 – 20 2014, Berlin, Germany*, GFaI, e.V., Berlin, 2014.

[34] Dougherty, R. P., "Functional Beamforming for Aeroacoustic Source Distributions," 20^{th} *AIAA/CEAS Aeroacoustics Conference. June 16 – 20 2014. Atlanta GA, USA*, 2014, AIAA paper 2014–3066.

[35] Snellen, M., Merino-Martinez, R., and Simons, D. G., "Assessment of noise level variability on landing aircraft using a phased microphone array," *Journal of Aircraft*, 2016, Accepted for publication (doi: 10.2514/1.C033950).

[36] Camier, C., Padois, T., Provencher, J., Gauthier, P.-A., Berry, A., Blais, J.-F., Patenaude-Dufour, M., and Lapointe, R., "Fly–over source localization on civil aircraft," 19^{th} *AIAA/CEAS Aeroacoustics Conference. May 27 – 29 2013. Berlin, Germany*, 2013, AIAA paper 2013–2261.

[37] Dougherty, R. P., "Cross Spectral Matrix Diagonal Optimization," 6^{th} *Berlin Beamforming Conference, February 29 – March 1, 2016, Berlin, Germany*, GFaI, e.V., Berlin, 2016.

[38] Fink, M. R., "Noise component method for airframe noise," 4^{th} *AIAA Aeroacoustics Conference. October 3 – 5 1977, Atlanta, Georgia, USA*, 1977, AIAA Paper 1977–1271.

[39] Guo, Y., "Empirical Prediction of Aircraft Landing Gear Noise," Tech. Rep. NASA TM–2005–213780, 2005.

[40] Aures, W., "Procedure for calculating the sensory euphony of arbitrary sound signal," *Acustica*, Vol. 59, No. 2, 1985, pp. 130–141.

[41] Sahai, A. K. and Stumpf, E., "Incorporating and Minimizing Aircraft Noise Annoyance during Conceptual Aircraft Design," 20^{th} *AIAA/CEAS Aeroacoustics Conference, June 16 – 20 2014, Atlanta, GA, USA*, 2014, AIAA paper 2014–2078.

[42] Sahai, A. K., *Consideration of Aircraft Noise Annoyance during Conceptual Aircraft Design*, Ph.D. thesis, Rheinisch–Westfälische Technische Hochschule Aachen, 2016.